SOPHION BIOSCIENCE | Discover more

# Application Report

## High-throughput evaluation of cardiac safety targets $Na_V1.5$ and $Ca_V1.2$ in axoCells™ hiPSC-derived cardiomyocytes using Qube 384

Sample $Na_V1.5$ compound screen and an initial evaluation of perforated patch as a strategy for $Ca_V1.2$ and action-potential recordings in axoCells™ hiPSC-derived ventricular cardiomyocytes.


## Summary

This study demonstrates the capability of Qube 384 as a reliable and robust platform for electrophysiological characterization of axoCells™ Human iPSC-derived Ventricular Cardiomyocytes(hiPSC-CMs). Qube 384 supports whole-cell and perforated voltage- and current-clamp recordings, enabling high-throughput cardiotoxicity and/or drug testing.

The results include:

- axoCells™ hiPSC-CMs assay with whole-cell (WC) success rate of above 80%.
- axoCells™ hiPSC-CMs assay for $Na_V1.5$ compound screening running with a 60% success rate
- Proof-of-concept perforated patch recordings of $Ca_V1.2$ currents and action-potentials in axoCells™ hiPSC-CMs


## Introduction

Cardiac ion channels present highly attractive therapeutic targets in the cardiovascular system. They are also a major factor in drug-induced cardiotoxicity. This makes electrophysiological studies of hiPSC-CMs vital to their usage in drug discovery and safety studies.

However, historically, these studies have been limited by the labour-intensive and low-throughput nature of manual patch-clamp electrophysiology. In addition, limitations in the technique have impacted the quality of the data obtained, challenging its physiological relevance.

This study aims to demonstrate the utilisation of Sophion's Qube 384 automated patch clamp (APC) platform for high-throughput electrophysiological characterisation and compound screening of cardiac safety targets, $Na_V1.5$ and $Ca_V1.2$, in axoCells™ hiPSC-derived ventricular CMs.

In addition, it aims to demonstrate the possibility of using perforated patch clamp recordings to increase the physiological relevance of $Ca_V1.2$ and action-potential measurements.

The possibility of performing perforated patch-clamp recordings of hiPSC-derived CMs on an APC platform, as demonstrated in the proof-of-concept experiments here, opens a new avenue for more physiologically relevant and improved pharmacological studies due to:

- Preservation of the intracellular signaling
- Reduced current rundown
- Limited fluoride-related artifacts

## Results and discussion

### Biophysical and pharmacological evaluation of $Na_V$ currents on Qube 384

To assess the electrophysiological properties of axoCells™ hiPSC-CMs, patch-clamp recordings were performed on Qube 384, with cell and channel properties presented in Figure 1. The hiPSC-CMs displayed a heterogenous cell size distribution with capacitance ($C_{slow}$) and membrane resistance ($R_{mem}$) values within the expected range for hiPSC-derived CMs at this stage of development[1] (mean $C_{slow}$ = 9.5 pF and mean $R_{mem}$ = 1.5 GΩ, Figure 1C and D). The whole-cell success rate was 84% ± 4%, as illustrated in Figure 1A and B, and in 66% ± 3% of the experiment sites, we recorded $Na_V$ currents with amplitude greater than or equal to 200 pA (Figure 1A and B).

The IV relationship for $Na_V1.5$ shows peak sodium current at ~ -10 mV (Figure 1F), in line with literature values[2]. In addition, the membrane potential at which 50% of the $Na_V1.5$ channels are activated, i.e. $V_{half}$ of activation, was -33 mV ± 8 mV for the hiPSC-CMs (Figure 1G), in line with literature values of ~ -35 mV for $Na_V1.5$ recorded in cardiac tissue ventricular-like CMs specifically[2]. Similarly, the $V_{half}$ of inactivation for cardiac tissue and ventricular-like CMs was shown to be ~ -75 mV[2], which aligns with a $V_{half}$ of inactivation = -72 mV ± 6 mV that was found in this study (Figure 1G).

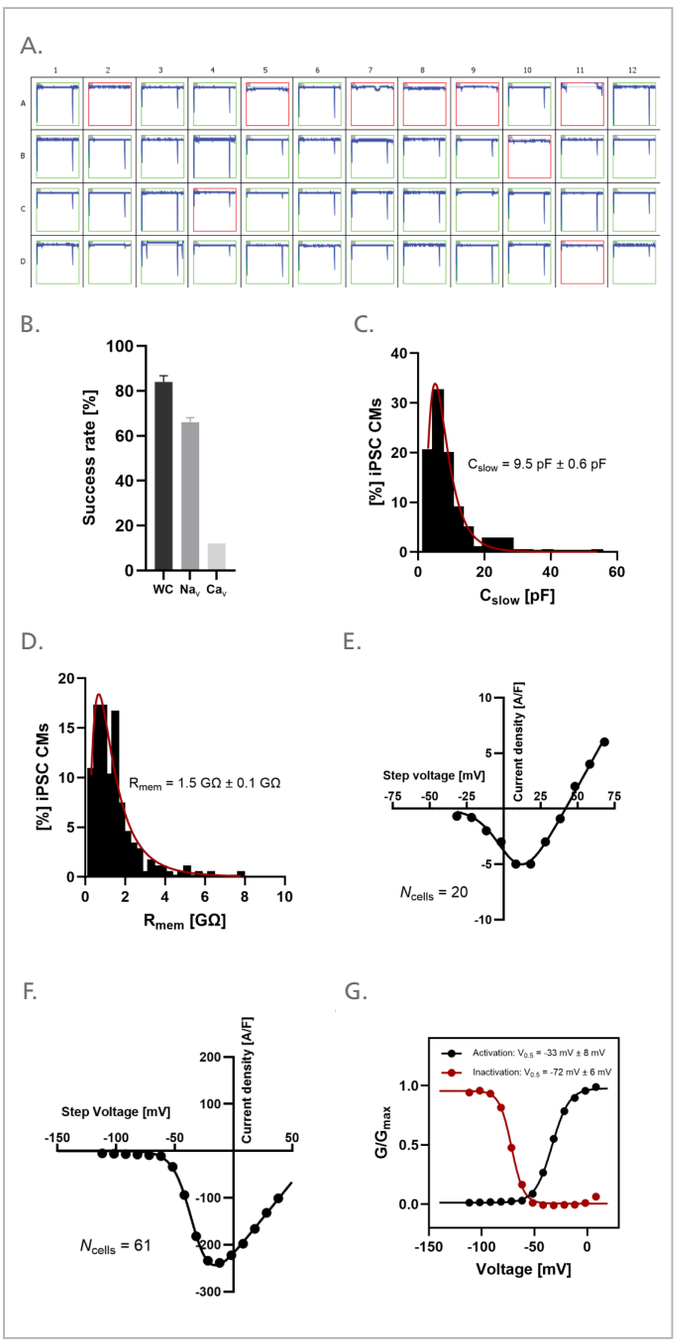


**Fig. 1: A) Performance of axoCells™ hiPSC-CMs on Qube 384.** Plate view (48 out of 384 experiment sites) displaying $Na_V$ currents recorded in hiPSC-CMs. Green and red framed are the experiments that pass and fail the quality filter, respectively. **B)** Experiment success rates plotted for whole-cell (WC) (dark grey); $Na_V$ current (grey) and $Ca_V$ current (light grey) in percentage of experiment sites. Note that due to low cell numbers, hiPSC-CMs were only added in half a measurement plate (192 experiment sites). Data is mean ± SEM of one or two measurement plates. **C)** and **D)** Histograms of $C_{slow}$ and $R_{mem}$ values of the measured cell population ($N_{cells}$ = 177) and best fit of the distribution (red line). **E)** $Ca_V$ current density vs. step voltage plot. Data points are mean ± SEM of 20 cells. **F)** $Na_V$ current density vs. step voltage plot. Data points are mean ± SEM of 61 cells. **G)** Normalized conductance vs voltage plotted for $Na_V$ activation (black) and inactivation (red). Fit of the Boltzmann equation resulted in a $V_{half}$, act and $V_{half}$, inact of approximately – 33 mV and -72 mV, respectively, in line with reported values for $Na_V1.5$[2].

For further electrophysiological evaluation of axoCells™ hiPSC-CMs, a sample compound dose-response was performed using the well-known state-dependent $Na_V$ blocker, tetracaine, as an example of a $Na_V1.5$ compound screen (Figure 2).

$Na_V$ peak currents were recorded in hiPSC-CMs upon the addition of 0.3 % DMSO (control, grey, Figure 2A ) or increasing concentrations of tetracaine (5 point, 10-fold dilution from 100 µM, orange, Figure 2A) using a two-pulse activation protocol to -10 mV (Figure 2B). The second pulse was applied after clamping the CM at $V_{half}$, the membrane potential at which 50% of the $Na_V1.5$ channels are activated, which was adaptively recorded for each individual cell via the adaptive $V_{half}$ functionality in Qube 384 (Figure 2B).

Subsequently, the normalized $Na_V$ peak currents, recorded both in response to the first and second activation pulse, were plotted as a function of tetracaine concentration. Based on the Hill equation, the $IC_{50}$ values for peak 1 and peak 2 were calculated to be ~25 µM and ~2.8 µM, respectively, which is in line with previous comparable studies for $Na_V1.5$[2].

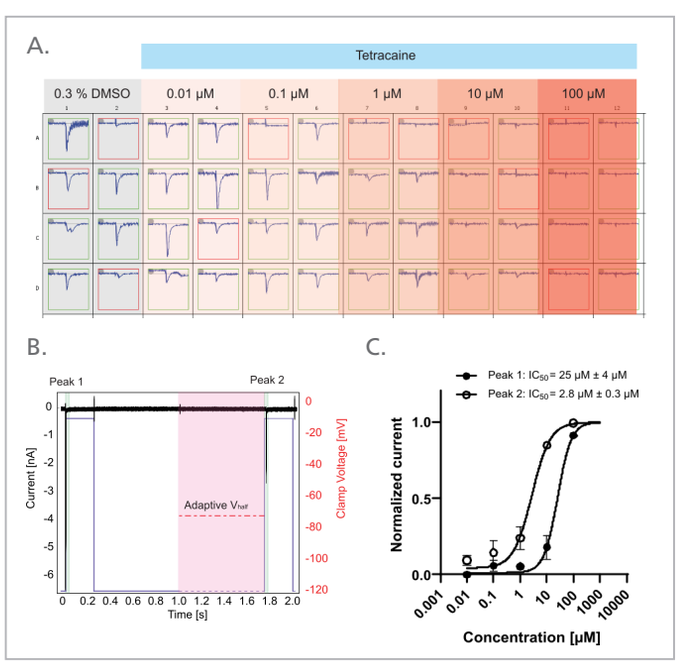


**Fig. 2: $Na_V$ blocker concentration-response experiment using axoCells™ hiPSC-CMs on Qube 384. A)** Plate view (48 out of 384 experiment sites) displaying $Na_V$ peak currents recorded in hiPSC-CMs upon the addition of 0.3 % DMSO (control, grey) or increasing concentrations of the state-dependent $Na_V$ blocker tetracaine (5 point 10-fold dilution from 100 µM, orange). Green and red framed current traces are the experiments that pass and fail the $Na_V$ current filter, respectively. **B)** The two-pulse protocol used to evaluate the state-dependent blocker, consisting of two 0.2 s pulses, from -120 mV to -10 mV, separated by 1.6 s in total, 0.8 s at -120 mV and 0.8 s at the $V_{half}$ value recorded adaptively for each single cell. **C)** Normalized $Na_V$ peak current as a function of tetracaine concentration plotted for peak 1 (solid black) and peak 2 (black outline), respectively. Fitting of the Hill equation resulted in $IC_{50}$ values of approximately 25 µM and 2.8 µM, for peak 1 and peak 2 respectively, in line with previous comparable studies for $Na_V1.5$[2].

## Biophysical evaluation of $Ca_V$ currents on Qube 384

The percentage of experiment sites, in which we could detect $Ca_V1.2$ currents, was lower, with a success rate of ~12% (Figure 1B). However, in the cells with $Ca_V1.2$ current, the latter peaked at voltages ~ +10 mV (Figure 1E), which is in line with electrophysiological studies of $Ca_V1.2$ in CMs[4]. The lower success rate of the $Ca_V1.2$ current is expected when seal-enhancing solutions (containing $F^-$) are used alongside standard whole-cell (WC) protocols. This is the result of the $F^-$ precipitating free intracellular $Ca^{2+}$, which is essential for proper $Ca_V1.2$ channel function.

To circumvent the issues associated with measuring consistent and stable $Ca_V1.2$ currents in CMs, perforated patch-clamp recordings were evaluated as an alternative (Figure 3). Perforation of the cell membrane, rather than its rupture, helps preserve the intracellular environment by limiting the washout of key signaling molecules. In addition, it avoids direct exposure of the intracellular environment to fluoride. Thus, it is hypothesized that perforated patch-clamp could help in optimizing and maintaining stable $Ca_V1.2$ currents.

Figure 3 shows the comparison of the $Ca_V1.2$ IV plots and the action potential duration at 90% of repolarization ($APD_{90}$) between the standard whole-cell (std WC, N = 5 cells) and the perforated cell configuration (N = 10 cells). The averaged $Ca_V$ IV plots for the std WC and the perforated configuration show maximal $Ca_V$ current at ~0 mV and activation threshold of ~ -40 mV (Figure 3A). This is also in line with previous observations in iPSC-derived CMs[4,5] and with previously reported data on Qube for $Ca_V1.2$[6]. As observed with the perforated mode, the peak $Ca_V1.2$ current at ~ 0 mV is visibly larger than the peak current at the std WC configuration (Figure 3A and B). The reversal potential for $Ca_V1.2$ is also in line with the reported for iPSC-derived CM reversal potentials between +60 mV and +80 mV[1,2] (Figure 3A) and ~ +50 mV for Qube $Ca_V1.2$ recordings[6,7].

Using adaptive current-clamp recordings ($I_{adapt}$), it was possible to record evoked action potentials (APs) in the hiPSC-derived CM (Figure 3). Comparison of the shape of the APs in whole-cell vs perforated patch-clamp, prior to and after addition of the perforating agent nystatin, demonstrates the effects of perforation on the AP duration (APD) (Figure 3C). There is a clear increase when perforated current clamp is applied in comparison to whole-cell current clamp (Figure 3D).

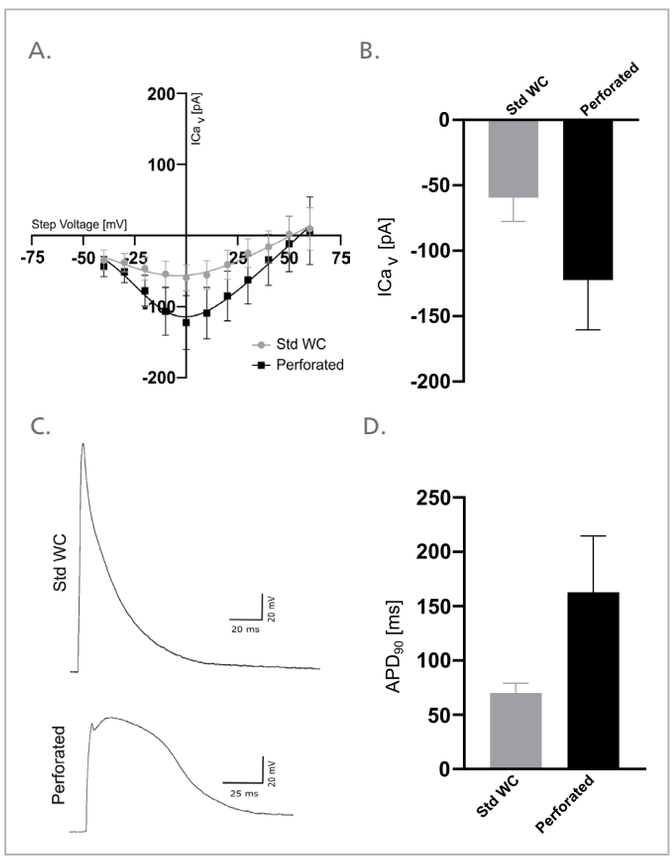


**Fig. 3: Proof-of-concept standard WC vs perforated patch-clamp in axoCells™ hiPSC-CMs on Qube 384. A)** $Ca_V$ current vs step voltage plot recorded using standard whole-cell (grey) and perforated (black) patch-clamp. Data points are mean ± SEM of 5 cells (std WC) and 10 cells (perforated). **B)** Bar diagram of maximum $Ca_V$ current recorded using Std WC (grey) and perforated (black) patch-clamp. **C)** Representative traces of paced action potentials acquired using standard whole-cell (upper) and perforated (lower) patch-clamp. **D)** Bar diagram of $APD_{90}$ values using std WC (grey) and perforated (black) current-clamp recordings.

## Conclusion

This study shows that axoCells™ hiPSC-CMs can be assessed using Qube 384 with whole-cell success rates of above 80%, thus demonstrating suitable technologies for $Na_V$ current screening, with current success rates of above 60%.

Perforated patch of hiPSC-CMs is challenging and requires additional optimization to achieve success rates that are relevant for screening purposes. However, the proof-of-concept perforated patch recordings presented here, suggest this configuration as an alternative strategy to standard whole-cell, for recordings of $Ca_V1.2$ currents and action potentials. Given further optimization, this could offer the possibility of more physiologically relevant recordings of these cardiac targets.

## Methods

- Human iPSC-derived Ventricular Cardiomyocytes (CM) were kindly provided by Axol Bioscience, and cultured according to manufacturer protocols until the day of experiment.

- For information on dissociation procedures and solutions contact us at info@sophion.com.

## References


1. Ma J, *et al.* (2011) High purity human-induced pluripotent stem cell-derived cardiomyocytes: electrophysiological properties of action potentials and ionic currents. **Am J Physiol Heart Circ Physiol**.
2. Karatsiompani, S and Badone, B (2022) hiPSC-derived cardiomyocytes – $Na_V1.5$ compound screening on QPatch II. **Sophion Application Report**
3. Mesirca P *et al.* (2024) Selective blockade of $Ca_V1.2$ (α1C) versus $Ca_V1.3$ (α1D) L-type calcium channels by the black mamba toxin calciseptine. **Nat Commun**.
4. Uzun AU *et al*. (2016) Ca(2+)-Currents in Human-Induced Pluripotent Stem Cell-Derived Cardiomyocytes Effects of Two Different Culture Conditions. **Front Pharmacol**
5. Zhang XH *et al*. (2015) Regionally diverse mitochondrial calcium signaling regulates spontaneous pacing in developing cardiomyocytes. **Cell calcium**
6. Melanie Schupp (2019) $Ca_V1.2$ on Qube 384 - pharmacology, stability and CiPA. **Sophion Application Report**
7. Reyes AD (2019) A breakthrough method that became vital to neuroscience. **Nature**



**Author:**

Atanaska Velichkova, Research scientist

Kadla R. Rosholm, Sr. Research Scientist



Human iPSC-derived Ventricular Cardiomyocytes (CM) were kindly provided by

AXOL

Contact: operations@axolbio.com



Sophion Bioscience A/S

info@sophion.com

sophion.com